



# HHS Public Access

Author manuscript

*J Am Chem Soc.* Author manuscript; available in PMC 2015 June 25.

Published in final edited form as:

*J Am Chem Soc.* 2003 May 14; 125(19): 5745–5753. doi:10.1021/ja034162h.

## Mithramycin SK, A Novel Antitumor Drug with Improved Therapeutic Index, Mithramycin SA, and Demycarosyl-mithramycin SK: Three New Products Generated in the Mithramycin Producer *Streptomyces argillaceus* through Combinatorial Biosynthesis

Lily L. Remsing<sup>†</sup>, Ana M. González<sup>‡</sup>, Mohammad Nur-e-Alam<sup>†</sup>, M. José Fernández-Lozano<sup>‡</sup>, Alfredo F. Braña<sup>‡</sup>, Uwe Rix<sup>†</sup>, Marcos A. Oliveira<sup>†</sup>, Carmen Méndez<sup>‡</sup>, José A. Salas<sup>‡</sup>, and Jürgen Rohr<sup>†</sup>

Division of Pharmaceutical Sciences, College of Pharmacy, University of Kentucky, 907 Rose Street, Lexington, Kentucky 40536-0082, and Departamento de Biología Funcional e Instituto Universitario de Oncología del Principado de Asturias (I.U.O.P.A), Universidad de Oviedo, 33006 Oviedo, Spain

José A. Salas: jasf@sauron.quimica.uniovi.es; Jürgen Rohr: jrohr2@uky.edu

### Abstract

To gain initial structure–activity relationships regarding the highly functionalized pentyl side chain attached at C-3 of mithramycin (MTM), we focused on a post-polyketide synthase (post-PKS) tailoring step of the MTM biosynthesis by *Streptomyces argillaceus* ATCC 12956, which was proposed to be catalyzed by ketoreductase (KR) MtmW. In this last step of the MTM biosynthesis, a keto group of the pentyl side chain is reduced to a secondary alcohol, and we anticipated the generation of an MTM derivative with an additional keto group in the 3-side chain. Insertional inactivation of *mtmW*, a gene located ca. 8 kb downstream of the mithramycin-PKS genes, yielded an *S. argillaceus* mutant, which accumulated three new mithramycin analogues, namely mithramycin SA, demycarosyl-mithramycin SK, and mithramycin SK (MTM-SK). The structures of these three compounds confirmed indirectly the proposed role of MtmW in MTM biosynthesis. However, the new mithramycin derivatives bear unexpectedly shorter 3-side chains (ethyl or butyl) than MTM, presumably caused by nonenzymatic rearrangement or cleavage reactions of the initially formed pentyl side chain with a reactive  $\beta$ -dicarbonyl functional group. The major product, MTM-SK, was tested in vitro against a variety of human cancer cell lines, as well as in an in vitro toxicity assay, and showed an improved therapeutic index, in comparison to the parent drug, MTM.

---

Correspondence to: José A. Salas, jasf@sauron.quimica.uniovi.es; Jürgen Rohr, jrohr2@uky.edu.

<sup>†</sup>University of Kentucky.

<sup>‡</sup>Universidad de Oviedo.

## Introduction

Mithramycin (MTM, **1**, also known as aureolic acid, mithracin, LA-7017, PA-144, and plicamycin; see Figure 1) is an aureolic acid-type polyketide produced by various soil bacteria of the genus *Streptomyces*, including *Streptomyces argillaceus* (ATCC 12956).<sup>1–3</sup> The aureolic acid group of anticancer antibiotics includes MTM, chromomycin A<sub>3</sub> (CHR), olivomycin A (OLI), UCH9, and the newly discovered durhamycin A.<sup>1,4,5</sup> All contain the same tricyclic core moiety with a unique dihydroxy-methoxy-oxo-pentyl side chain attached at C-3 and vary only slightly, with respect to the residue at C-7, which is either a H atom or a small alkyl side chain. However, these naturally occurring aureolic acid antibiotics differ in the nature and linking of their saccharide chains, which consist of various 2,6-dideoxysugar residues. Such structural variations impart subtle differences in the DNA binding and activity profiles among the members of this group.<sup>1,6–9</sup> MTM has been used clinically in the United States to treat Paget's disease and testicular carcinoma.<sup>10–13</sup> In addition, MTM's hypocalcemic effect has been used to manage hypercalcemia in patients with malignancy-associated bone lesions.<sup>14</sup> Unfortunately, it exhibits severe side effects, such that the current clinical use of MTM is limited by its gastrointestinal, hepatic, renal, and bone marrow toxicities, which result in nausea, vomiting, and bleeding.<sup>11,15</sup> Consequently, it is important to investigate MTM analogues for increased therapeutic indexes.

MTM interacts with the minor groove of DNA, mainly in GC-rich regions, as a 2:1 MTM:Mg<sup>2+</sup> complex, cross-linking the DNA and blocking its template activity for DNA- and RNA-dependent polymerases, thereby inhibiting replication and transcription processes.<sup>6</sup> The specific characteristics of the DNA: antibiotic interaction have been intensively investigated by NMR and X-ray crystallographic studies,<sup>8,9,16–18</sup> particularly in view of the role played by the oligosaccharide moieties. These and other studies revealed that the C–D units of the trisaccharide chains of MTM, OLI, and CHR stack on the aromatic core of the dimer-partner aglycon, and that the intact C–D–E trisaccharide moiety is essential for dimer formation as well as optimal DNA binding. The role of the C-3 polyoxygenated pentyl side chain is not well characterized, except through the X-ray structure of the MTM–DNA complex,<sup>8,9</sup> which reveals that the pentyl side chain interacts with the phosphate backbone of the DNA, leading to the hypothesis that modifications of this alkyl side chain may be profitable. Thus, derivatives, which differ from their parent drug, with respect to the alkyl side chain at C-3, are needed to further investigate structure–activity relationships of the aureolic acid-type antitumor drugs.

Synthetic and semisynthetic approaches toward the production of new aureolic acid-type compounds are complemented by combinatorial biosynthetic procedures, whereby the genes of the biosynthetic pathway of the drugs are altered in the bacteria themselves (e.g., through gene inactivation, expression, or recombination). This method not only allows the generation of new derivatives, the so-called “unnatural natural compounds”, but also simultaneously generates a bacterial strain, which allows the biotechnological mass production of the new derivative. The biosynthetic gene cluster leading to the formation of MTM has been studied in our laboratories over the last years and resulted in the identification of 34 genes and the assignment of various gene product functions for the



Upon transformation of the wild-type *S. argillaceus* ATCC 12956 with pM7W1, transformants were selected for their resistance to apramycin. One of these transformants, named mutant M7W1, was found to be also sensitive to thioestrepton, being the consequence of a double crossover, which results in the replacement of the wild-type gene by the in vitro mutated one. This fact was confirmed by Southern hybridization: the 4.5 kb *Bam*HI fragment of the wild-type strain was replaced by two new *Bam*HI fragments of 3.7 and 2.3 kb, as expected if the replacement occurred. It was also confirmed that the gene replacement only affected *mtmW*, because expressing this gene in trans, using pAGW, restored MTM production in mutant M7W1.

### Isolation and Structure Elucidation of the Novel Compounds

*S. argillaceus* M7W1 was grown on a R5A liquid medium and, after 5 days of incubation, the culture supernatant was subjected to solid-phase extraction. The material eluted with a methanol:water mixture was analyzed by reverse-phase HPLC. No MTM production was detected. However, two new HPLC peaks were detected. The absorption spectra of the compounds present in these two peaks were characteristic of MTM biosynthetic intermediates in which the opening of the fourth ring had occurred.<sup>24</sup> The compounds in these two peaks were purified, with yields of 14.5 mg/L for the major compound (MTM-SK) and 2.2 mg/L for the minor compound (demyc-MTM-SK) (Figure 3). Alternatively, a liquid extraction work-up procedure, followed by conventional chromatography, was used to isolate the new compounds. Following acidification to pH 5.5, the culture was extracted using (i) EtOAc and (ii) *n*-BuOH. The more-lipophilic compounds, MTM-SK (yield of 9 mg/L) and demyc-MTM-SK (yield of 2 mg/L), were found in the EtOAc extract, whereas the more-hydrophilic MTM-SA (yield of 5 mg/L, Figure 3) was solely found in the *n*-BuOH extract. Silica gel chromatography was used for both the EtOAc extract and the *n*-BuOH extract. MTM-SK and demyc-MTM-SK were finally purified using an RP-18 silica gel column, followed by Sephadex-LH 20 chromatography. MTM-SA was finally purified through preparative thin-layer chromatography (TLC), using RP-18 silica gel plates. The exact isolation procedure is described in the discussion regarding the feeding experiments in the Experimental Section.

The structures of the new compounds were elucidated using physicochemical methods. The <sup>1</sup>H NMR and <sup>13</sup>C NMR spectra (Table 1), in combination with the positive-mode electrospray ionization (ESI) mass spectrum, which revealed a molecular ion of *m/z* 1077.4 (M + Na<sup>+</sup>), indicated the molecular formula of the major compound to be C<sub>51</sub>H<sub>74</sub>O<sub>23</sub> (MW = 1054.4). This was verified by high-resolution positive-mode fast atom bombardment mass spectroscopy (FAB MS) (HR for C<sub>51</sub>H<sub>74</sub>O<sub>23</sub>-Na: calcd, 1077.4519; observed, 1077.4478). The presence of five anomeric carbon signals ( $\delta_C$  97.0, 97.9, 99.9, 100.3, and 100.8) and the analysis of the additional sugar <sup>1</sup>H NMR and <sup>13</sup>C NMR chemical shifts and coupling constants indicated that the typical MTM glycosylation pattern was upheld. Specifically, a diolivose is attached to the C-6 position of the aglycon and a trisaccharide composed of an olivose, an oliose, and a mycarose moiety is attached at C-2. All are  $\beta$ -glycosidically linked (10-Hz transaxial coupling between the 1-H and 2-H<sub>a</sub>) with the interglycosidic connections, as well as the points of linkage to the aglycon, clearly assigned from the heteronuclear multiple bond connectivity (HMBC) spectra. Also, as in MTM, the aglycon is methylated at

the C-7 position ( $\delta_C$  7.9,  $\delta_H$  2.15). The difference between this compound and MTM lies in the side chain at C-3, which is unexpectedly missing one hydroxylated carbon (a difference of 30 amu from MTM). The novel hydroxy-methoxy-oxo-butyl side chain in MTM-SK bears the typical 1'-OCH<sub>3</sub> group ( $\delta_C$  60.0,  $\delta_H$  3.55), a hydroxylated carbon at the 2'-position ( $\delta_C$  79.46,  $\delta_H$  4.32), a keto group in the 3'-position ( $\delta_C$  209.9), and terminates with a methyl group ( $\delta_C$  26.3,  $\delta_H$  2.35). This is supported by the coupling pattern associated with the protons of this side chain. In particular, H-1', which is normally a simple doublet, being situated between H-3 and the 2'-keto group of MTM, is now a doublet of a doublet, as would be expected if the keto function at 2' had been replaced by a carbon bearing a single proton. Furthermore, the methyl group, which ends the side chain, is now a sharp singlet instead of a doublet and its carbon and proton signals are shifted downfield ( $\delta_C$  26.26,  $\delta_H$  2.35), compared to those found in the normal MTM compound ( $\delta_C$  18.7,  $\delta_H$  1.26), indicative of its proximity to the keto group at C-3'. Important HMBC couplings substantiating this structure include the  $^4J_{C-H}$  couplings between C-2' and H-2 and 1'-OCH<sub>3</sub> and the  $3J_{C-H}$  couplings between C-2 and H-1', C-3 and H-2', C-2' and H<sub>3</sub>-4', and C-3' and H-1'. Other typical MTM HMBC couplings were similar to those recently published.<sup>28</sup> Thus, the major compound is MTM-SK (**2**), where SK refers to the shortened side chain with a relocated keto function. The suggested stereochemistry of the center at C-2' shown in the structure for **2** follows from semiempirical calculations, which propose a hydrogen bond between 2'-OH and 2-O. Only the structure with *R*-configuration at C-2' in such an arrangement is in agreement with the NMR data (the dihedral angle between 1'-H and 2'-H is ca. 30°, in agreement with  $J_{1'-H/2'-H} = 3.4$  Hz), whereas for the molecule with the opposite stereochemistry at C-2', a dihedral angle of ~180° was found.<sup>33</sup>

The positive-mode ESI mass spectrum of the second compound revealed a molecular ion of  $m/z$  933.4 (M + Na<sup>+</sup>), indicating the molecular formula to be C<sub>44</sub>H<sub>62</sub>O<sub>20</sub> (MW = 910.4), which is seven carbon atoms less than that found for MTM-SK. This was verified by high-resolution positive-mode FAB MS (HR for C<sub>44</sub>H<sub>62</sub>O<sub>20</sub>K: calcd, 949.3472; observed, 949.3482). The presence of only four anomeric carbon signals ( $\delta_C$  97.1, 99.9, 100.4, and 100.8) and, in particular, the nonappearance of the 3E quaternary carbon and the 3E methyl group indicated that the loss of seven carbon atoms was due to the absence of the mycarose moiety normally attached to the 3-position of oliose. Further analysis of the <sup>1</sup>H NMR and <sup>13</sup>C NMR spectra (see Experimental Section) indicated that the remaining structural features, including the shortened side chain, were identical to MTM-SK; thus, the minor compound was deduced to be demyc-MTM-SK (**3**). Demycarosyl-mithramycin derivatives have been isolated only once before;<sup>28</sup> thus, demyc-MTM-SK provides further evidence for the flexibility of the enzymes, which normally act following the addition of the mycarose moiety, e.g., MtmGI, MtmGII, and MtmOIV.<sup>34</sup> The missing mycarose moiety in **3** might also reflect the possibility that the inactivation of *mtmW* slightly compromised the function of the product of the gene immediately downstream, *mtmGIV*, which encodes the glycosyltransferase responsible for the attachment of the D-mycarose unit in the mithramycin biosynthesis.<sup>28,35</sup>

The negative- and positive-mode ESI mass spectrum of the third compound, which was only obtained following a liquid extraction procedure, showed a molecular ion of  $m/z$  1025.4 (M

$-H)^-$  and  $m/z$  1049.4 ( $M + Na^+$ ), respectively, indicating the molecular formula to be  $C_{49}H_{70}O_{23}$  (MW = 1026.4). The analysis of  $^1H$  NMR,  $^{13}C$  NMR, and various two-dimensional (2D) NMR spectra indicated that all structural features of this minor product were identical to those of MTM-SK (**2**), except the 3-side chain (see Experimental Section). The  $^1H$  signals corresponding to the 4' methyl group and the H-2' of the 3-side chain were missing in the  $^1H$  NMR analysis, whereas the  $^{13}C$  NMR analysis confirmed the absence of carbons C-3' and C-4'. The  $^{13}C$  NMR analysis showed a characteristic new carbonyl carbon at  $\delta$  176.8, indicating C-2' to be a carboxylic acid. Thus, the compound isolated from the *n*-BuOH extract of the MTM-SK producer possesses a very short 3-side chain ending with a carboxylic acid group at the 2'-position and was consequently named mithramycin SA (MTM-SA (**4**), for short side chain and acid). It is possible that **4** is (partly) an artifact of the work-up procedure, because its formation from the putative labile compound **5** (see below) is acid-catalyzed, and the culture needed to be adjusted to a slightly acidic pH (5.5) to enable the extraction of **4** into the organic phase. On the other hand, this minor compound may have been missed in the work-up procedure following solid extraction, because it might have gotten absorbed onto the HPLC column.

### Rearrangement Reactions and Incorporation Experiments

The structures of MTM-SK (**2**) and its demycarosyl derivative **3** were intriguing, because we expected compound **5** to be accumulated from the inactivation of ketoreductase MtmW. However, compound **5** has a highly functional and, thus, reactive 3-side chain, which contains two keto functions in the  $\beta$ -position, relative to each other, separated by a carbon atom bearing another oxygen atom. This  $\beta$ -dicarbonyl constellation might trigger a Favorskii-like rearrangement (Figure 4A), for which an 1,2-acyl shift induced by deprotonation of the central alcohol can be envisaged, followed by the addition of water on the resulting aldehyde and a consequent departure of formic acid. Moore and co-workers recently discussed a similar Favorskii-type rearrangement, in regard to the enterocin biosynthesis; however, there, the reaction occurs after an oxidative cleavage of a C-C bond and therefore is more likely to be enzymatically catalyzed.<sup>36,37</sup> MTM-SA (**4**) also gives indirect evidence for the labile structure **5**, because its formation from **5** is possible through the attack of water at the carbonyl adjacent to the methoxy group, followed by retro-aldol cleavage to yield MTM-SA (**4**) and hydroxyacetone (Figure 4B).

To prove the excision of carbon 3', two feeding experiments using  $[1-^{13}C]$ -acetate and  $[1,2-^{13}C_2]$ -acetate were performed (Table 1). The oxidative rearrangement during the biosynthesis of MTM leads to an acetate incorporation pattern, shown in Figure 5, in which carbons 4' and 5' of the 3-side chain stem from the starter unit, whereas carbons 1', 2', and 3' were once the end of the polyketide chain.<sup>3,38</sup> If C-3' is lost, two intact acetate units "facing each other" from opposite directions should result. The results, also shown in Figure 5, are consistent with these expectations and, thus, prove the loss of carbon 3'.

Although we favor the nonenzymatic rearrangement reaction previously shown for the formation of MTM-SK (**2**), a participation of an enzyme, especially an oxygenase, as discussed for the enterocin biosynthesis,<sup>37</sup> cannot be excluded. Therefore, alternative oxidative rearrangement mechanisms are also possible, for which either one of the

oxygenases of the *mtm* gene cluster<sup>3</sup> or any other *S. argillaceus* oxygenase might be responsible.

### Biological Activity

The antitumor activity of the two compounds was tested against a variety of tumor cell lines, including the 60 human tumor cell line assay of the NCI (National Cancer Institute, Bethesda, MD).<sup>39–41</sup> Compilation of the average log(GI<sub>50</sub>) values showed that both compounds were active, with MTM-SK (activity up to 9 times higher than that of MTM) being much more active than demyc-MTM-SK (ca. 25 times less active than MTM) (Table 2a). MTM-SK was particularly active against melanoma, leukemia, and CNS cancer cells (log(GI<sub>50</sub>) values of  $-7.64$ ,  $-7.59$ , and  $-7.61$ , respectively). Given the increased activity observed for **2**, a neutral red uptake analysis of squamous, melanoma, lung, and breast carcinomas was performed (Frevert<sup>42</sup>), which not only confirmed the increased activity of mithramycin SK as compared to MTM, but also showed an even more pronounced improvement of activity (up to ca. 90 times better) (Table 2b). In addition, toxicity assays using this same process and mouse 3T3 fibroblast (nontumor) cells showed that **2**, with an IC<sub>50</sub> value of  $1.96 \times 10^{-5}$  M, is more than 1500-fold less toxic than MTM (IC<sub>50</sub> values ranging from  $1.29 \times 10^{-8}$  to  $3.45 \times 10^{-9}$  M). (From Frevert,<sup>42</sup> Ginsburg et al.,<sup>43</sup> and Givens et al.<sup>44</sup>) Thus, MTM-SK (**2**) displays a significantly improved therapeutic index, up to 4 orders of magnitude better, compared to its parent drug, MTM.

## Experimental Section

### Microorganisms, Culture Conditions, and Plasmids

*Streptomyces argillaceus* ATCC 12956 was used as the source of chromosomal DNA. For sporulation on a solid medium, it was grown at 30 °C on plates containing medium A.<sup>47</sup> For protoplast transformation, it was grown in a YEME medium containing 17% sucrose. For growth in a liquid medium, the organism was grown in a TSB medium (trypticase soya broth, Oxoid). *Escherichia coli* XL1blue (Stratagene, Germany) was used as the host for plasmid propagation. When plasmid-containing clones were grown, the medium was supplemented with the appropriate antibiotics: thiostrepton, 25 µg/mL; tobramycin, 20 µg/mL; ampicillin, 100 µg/mL; or apramycin, 25 µg/mL. Plasmids pBSKT,<sup>21</sup> pIJ2921,<sup>48</sup> pIAGO,<sup>49</sup> and pEFBA (a pBSK derivative containing an apramycin resistance cassette; Ernestina Fernández, unpublished) were used for subcloning experiments.

### DNA Manipulation Techniques

Plasmid DNA preparations, restriction endonuclease digestions, alkaline phosphatase treatments, ligations, Southern hybridization, and other DNA manipulations were performed according to standard procedures for *E. coli*<sup>50</sup> and *Streptomyces*.<sup>51</sup>

### DNA Sequencing

Sequencing was performed on double-stranded DNA templates using the dideoxynucleotide chain-termination method.<sup>52</sup> Both DNA strands were sequenced with primers supplied in the kits or with internal oligoprimers (17-mer) using an ALF-express automatic DNA sequencer (Pharmacia Biotech). Computer-aided database searching and sequence analyses were

conducted using the University of Wisconsin Genetics Computer Group programs package (UWGCG)<sup>29</sup> and the BLAST program.<sup>53–55</sup>

### Insertional Inactivation

For inactivation of the *mtmW* gene, a 4.5 kb *Bam*HI fragment containing *mtmW*, *mtmGIV*, and portions of adjacent genes was subcloned into the *Bam*HI site of pBSKT, generating pM7W0. Then, an apramycin resistance cassette containing the *aac*(3)-IV gene was subcloned as a 1.5 kb *Sma*I-*Eco*RV fragment into the unique *Bgl*II site (blunt-ended) located within the coding region for *mtmW* and orientated in the direction of transcription of *mtmW*, thus generating pM7W1 (Figure 2). This construct was used to transform protoplasts of *S. argillaceus*. Transformants, in which the wild-type region of the chromosome was replaced by the in vitro mutated one through a double crossover at both sides of the apramycin cassette, were recognized by their resistance to apramycin and sensitivity to thiostrepton. The replacement was also verified by Southern analysis.

### Complementation of the *mtmW*-minus Mutant

A 1.1 kb *Xho*I-*Fsp*I fragment comprising the *mtmW* gene was subcloned into the *Sal*I-*Sma*I sites of pIJ2921, generating pAGW0. The gene was then rescued with *Sph*I (using the 5'-end *Sph*I site of the polylinker) and subcloned into the unique *Sph*I site of the bifunctional (*Streptomyces*-*E. coli*) plasmid pIAGO, immediately downstream of the erythromycin resistance promoter, *erm*Ep, generating pAGW. This construct was used for complementing the M7W1 mutant.

### Isolation of Compounds

A seed culture was prepared using TSB inoculated with spores of *S. argillaceus* M7W1 and incubated in an orbital shaker for 24 h at 30°C and 250 rpm. This seed culture was used to inoculate (at 2.5% v/v) eight 2-liter Erlenmeyer flasks, each containing 400 mL of R5A medium.<sup>47</sup> The flasks were incubated for 5 days under the previously described conditions. The entire culture obtained was centrifuged (12 000 rpm, 30 min), the pellets were discarded, and the supernatant was filtered (using membrane filters with a pore size of 0.45  $\mu$ m). The filtrate was applied to a solid-phase extraction cartridge (Supelclean LC-18, 10 g, Supelco), and the retained material was eluted with a mixture of methanol and water. A linear gradient from 0% to 100% methanol in 60 min, at 10 mL/min, was used. Fractions were taken every 5 min and, after HPLC analysis, the new compounds were found in fractions eluted between 40 and 55 min. These were evaporated under vacuum, redissolved in a mixture of dimethyl sulfoxide and methanol (50:50), and chromatographed using a  $\mu$ Bondapak C18 preparative column (PrepPak Cartridge, 25 mm  $\times$  100 mm, Waters), with acetonitrile (ACN) and water as solvents, at a flow rate of 10 mL/min. In the first step, a linear gradient from 30% to 50% ACN in 30 min was used. The material in the two peaks collected in this step was further purified under isocratic conditions with 37.5% ACN in water as a solvent. The isolated products were finally dried in vacuo and weighed.

An alternative work-up procedure via liquid extraction and conventional chromatography is described below (in the Feeding Experiments section).



## Feeding Experiments

A seed culture was prepared using TSB inoculated with spores of *S. argillaceus* M7W1 and incubated in an orbital shaker for 24 h at 30°C and 250 rpm. This seed culture was used to inoculate (at 2.5% v/v) sixteen 250-mL Erlenmeyer flasks, each containing 100 mL of modified R5 medium. Thirty-two hours after the inoculation, the pulse feeding of sodium acetate was started and continued for 36 h at 12-h intervals (four feedings for a total of 1 g of sodium acetate per liter of culture). For the single- and double-labeled experiments, **1**-<sup>13</sup>C and **1,2**-<sup>13</sup>C sodium acetate compounds, respectively, were used. The culture was then grown for an additional 52 h, for a total of 120 h before extraction. Following acidification with HCl to pH 5.5, the culture was extracted first with EtOAc and then with BuOH. The <sup>13</sup>C-labeled MTM-SK and demyc-MTM-SK were isolated from the EtOAc extract (0.21 g) using several chromatographic steps. The first step was a silica gel column (25 cm × 3 cm, eluted with CHCl<sub>3</sub> and MeOH, 9:1). The second column, an RP-18 silica gel column (11 cm × 1.75 cm), was eluted with water and ACN (65:35) being used to apply pressured air. Finally, MTM-SK and demyc-MTM-SK were purified using a Sephadex LH-20 column (100 cm × 2.5 cm, eluted with MeOH). Yields: MTM-SK, 13.7 mg; demyc-MTM-SK, 3.2 mg (both obtained as amorphous solids). MTM-SA was isolated from the BuOH extract (4.8 g), using (i) a silica gel column (25 cm × 3 cm, CHCl<sub>3</sub>:MeOH = 8.5:1.5), followed by (ii) a final purification via preparative TLC (20 cm × 20 cm RP-18 silica gel plates, Merck RP-18 F<sub>254</sub>, solvent system, water/ACN (65:35)). The yellow zone containing MTM-SA (*R<sub>f</sub>* = 0.43) was cut out, and the pure compound was obtained as an amorphous yellow solid by extraction with MeOH and evaporation to dryness.

## HPLC Analysis

Analyses were performed with a reversed-phase column (Symmetry C18, 4.6 cm × 250 mm, Waters), with ACN and 0.1% trifluoroacetic acid in water as solvents. A linear gradient from 10% to 100% ACN in 30 min, at a flow rate of 1 mL/min, was used. Detection and spectral characterization of peaks were made with a photodiode array detector and Millennium software, extracting bi-dimensional chromatograms at 280 nm.

## Structure Elucidation and Characterization

The structures of the new MTM derivatives were elucidated by NMR spectroscopy and mass spectrometry. The electrospray ionization mass spectra (ESI-MS) were acquired using a Finnigan MAT LCQ mass spectrometer. The high-resolution positive-mode fast atom bombardment mass spectrometry (FAB) spectra were acquired using a model VG70SQ double focusing magnetic sector MS instrument. The UV spectra were recorded on a Varian model CARY50 spectrophotometer, and IR spectra were obtained from a pure sample of KBr disks in a Bio-Rad model FTS3000MX FT-IR spectrometer. All NMR data, if not stated otherwise, were recorded in acetone-*d*<sub>6</sub>, using either 300 or 400 MHz Varian Inova equipment or a 500 MHz Bruker model DMX instrument. The NMR data for **2** are listed in Table 1; the NMR data for **3** and **4** are given below. All NMR assignments are based on H,H-COSY, HSQC, and HMBC spectra, allowing an unambiguous assignment of all NMR signals. For the semiempirical calculations, the generation of the two possible diastereoisomeric three-dimensional structures of MTM-SK was performed, using the

builder module of the InsightII software (Accelrys, 2000), on the basis of the known structure of MTM.<sup>2</sup> Energy minimizations were performed within the discovery module of the InsightII software, using force field CFF91 running on a Silicon Graphics computer (model O2).<sup>33</sup>

#### NMR and MS Analysis Data for Mithramycin SK, C<sub>51</sub>H<sub>74</sub>O<sub>23</sub> (2)

ESI-MS  $m/z$  (relative intensity) [M + Na<sup>+</sup>]: 1077.4 (100). HR-FAB  $m/z$  [M + Na<sup>+</sup>]: calcd, 1077.4519; found, 1077.4478. UV (MeOH)  $\lambda_{\max}$  ( $\epsilon$ ): 421.5 (10 600), 315.5 (7400), 285.0 (54 500) nm. FT-IR (KBr)  $\nu$ : 3423 (OH), 2974 (CH), 2931 (CH), 2883 (CH), 1712 (C=O), 1600 (C=O), 1521 (C=C), 1371, 1164, 1068 cm<sup>-1</sup>. <sup>1</sup>H NMR  $\delta$  and <sup>13</sup>C NMR  $\delta$  data are given in Table 1.

#### NMR and MS Analysis Data for Demycarosyl-mithramycin SK, C<sub>44</sub>H<sub>62</sub>O<sub>20</sub> (3)

ESI-MS  $m/z$  (relative intensity) [M + Na<sup>+</sup>]: 933.4 (100). HR-FAB  $m/z$  [M + K<sup>+</sup>]: calcd, 949.3472; found, 949.3482. UV (MeOH)  $\lambda_{\max}$  ( $\epsilon$ ): 421.5 (13 600), 315.9 (10 300), 285.0 (61 900) nm. FT-IR (KBr)  $\nu$ : 3413 (OH), 2974 (CH), 2931 (CH), 2884 (CH), 1710 (C=O), 1629 (C=O), 1580 (C=C), 1369, 1166, 1068 cm<sup>-1</sup>. <sup>1</sup>H NMR (500 MHz, acetone-*d*<sub>6</sub>,  $\delta$ ): 1.33 (d, 12H,  $J$  = 6 Hz, 6A-H<sub>3</sub>, 6B-H<sub>3</sub>, 6C-H<sub>3</sub>, and 6D-H<sub>3</sub>), 1.58 (ddd, 1H,  $J$  = 12, 12, 10 Hz, 2B-H<sub>a</sub>), 1.62 (ddd, 1H,  $J$  = 12, 12, 10 Hz, 2C-H<sub>a</sub>), 1.76 (ddd, 1H,  $J$  = 12, 12, 10 Hz, 2D-H<sub>a</sub>), 1.90 (ddd, 1H,  $J$  = 12, 12, 10 Hz, 2A-H<sub>a</sub>), 1.95 (ddd, 1H,  $J$  = 12, 5, 2 Hz, 2D-H<sub>e</sub>), 2.17 (s, 3H, 7-CH<sub>3</sub>), 2.21 (ddd, 1H,  $J$  = 12, 5, 2 Hz, 2B-H<sub>e</sub>), 2.34 (s, 3H, 4'-H<sub>3</sub>), 2.47 (overlap, 1H, 3-H), 2.49 (overlap, 1H, 2A-H<sub>e</sub>), 2.51 (overlap, 1H, 2C-H<sub>e</sub>), 2.99 (dd, 1H,  $J$  = 9, 9 Hz, 4B-H), 3.01 (overlap, 2H, 4-H<sub>e</sub>), 3.01 (dd, 1H,  $J$  = 9, 9 Hz, 4C-H), 3.08 (dd, 1H,  $J$  = 9, 9 Hz, 4A-H), 3.19 (dd, 1H,  $J$  = 16, 3 Hz, 4-H<sub>a</sub>), 3.35 (dq, 1H,  $J$  = 9, 6 Hz, 5C-H), 3.38 (dq, 1H,  $J$  = 9, 6 Hz, 5B-H), 3.54 (bs, 1H, 4D-H), 3.56 (s, 3H, 1'-OCH<sub>3</sub>), 3.56 (overlap, 1H, 5A-H), 3.58 (overlap, 1H, 3B-H), 3.69 (overlap, 1H, 3C-H), 3.71 (bq, 1H,  $J$  = 6 Hz, 5D-H), 3.78 (ddd, 1H,  $J$  = 12, 9, 5 Hz, 3A-H), 3.80 (ddd, 1H,  $J$  = 12, 5, 3 Hz, 3D-H), 4.24 (dd, 1H,  $J$  = 3.4, 1.5 Hz, 1'-H), 4.31 (d, 1H,  $J$  = 3.4 Hz, 2'-H), 4.69 (dd, 1H,  $J$  = 10, 2 Hz, 1D-H), 4.77 (d, 1H,  $J$  = 11.5 Hz, 2-H), 4.77 (dd, 1H,  $J$  = 10, 2 Hz, 1B-H), 5.14 (dd, 1H,  $J$  = 10, 2 Hz, 1C-H), 5.43 (dd, 1H,  $J$  = 10, 2 Hz, 1A-H), 6.94 (s, 2H, 5-H, and 10-H). <sup>13</sup>C NMR (125.7 MHz, acetone-*d*<sub>6</sub>,  $\delta$ ): 7.9 (7-CH<sub>3</sub>), 16.5 (C-6D), 17.6 (C-6B), 17.9 (C-6C and C-6A), 26.2 (C-4'), 28.3 (C-4), 35.2 (C-2D), 37.5 (C-2A), 37.9 (C-2C), 40.0 (C-2B), 43.8 (C-3), 60.0 (1'-OCH<sub>3</sub>), 68.9 (C-3D), 70.2 (C-4D), 71.3 (C-5D), 72.7 (C-5A and C-5C), 75.4 (C-4A), 75.7 (C-4C), 77.5 (C-4B), 78.1 (C-2), 79.3 (C-1'), 79.5 (C-2'), 81.3 (C-3A), 81.7 (C-3C), 97.1 (C-1A), 99.9 (C-1B), 100.4 (C-1D), 100.8 (C-1C), 101.7 (C-5), 108.0 (C-8a), 108.6 (C-9a), 111.1 (C-7), 117.1 (C-10), 137.0 (C-4a), 139.1 (C-10a), 156.1 (C-8), 160.0 (C-6), 165.4 (C-9), 203.6 (C-1), and 209.8 (C-3').

#### NMR and MS Analysis Data for Mithramycin SA, C<sub>49</sub>H<sub>70</sub>O<sub>23</sub> (4)

Positive-mode ESI-MS  $m/z$  (relative intensity) [M + Na<sup>+</sup>], 1049.4 (100); negative-mode ESI-MS  $m/z$  (relative intensity) [M - H]<sup>-</sup>, 1025.4 (100). UV (MeOH)  $\lambda_{\max}$  ( $\epsilon$ ): 421.5 (10 300), 316.9 (26 800), 284.5 (50 600) nm. FT-IR (KBr)  $\nu$ : 3443 (OH), 2924, (CH), 2853 (CH), 1739 (C=O), 1646 (C=O), 1457 (C=C), 1369, 1026, 823 cm<sup>-1</sup>. <sup>1</sup>H NMR (400 MHz, pyridine-*d*<sub>5</sub>,  $\delta$ ): 1.50 (s, 3H, 3E-CH<sub>3</sub>), 1.52 (d, 3H,  $J$  = 6.5 Hz, 6E-H<sub>3</sub>), 1.62 (d, 9H,  $J$  = 6.0

Hz, 6A-H<sub>3</sub>, 6C-H<sub>3</sub>, and 6D-H<sub>3</sub>), 1.68 (d, 3H, *J* = 6.0 Hz, 6B-H<sub>3</sub>), 1.77 (bt, 2H, *J* = 10.0 Hz, 2E-H<sub>a</sub> and 2B-H<sub>a</sub>), 1.92 (bdd, 1H, *J* = 12, 9 Hz, 2C-H<sub>a</sub>), 2.02 (bdd, 1H, *J* = 12, 11 Hz, 2D-H<sub>a</sub>), 2.08–2.22 (overlap, 2H, 2A-H<sub>a</sub>, and 2D-H<sub>e</sub>), 2.28 (dd, 1H, *J* = 9, 2 Hz, 2E-H<sub>e</sub>), 2.38 (bd, 1H, *J* = 10 Hz, 2A-H<sub>e</sub>), 2.47 (s, 3H, 7-CH<sub>3</sub>), 2.54 (m, 1H, 2C-H<sub>e</sub>), 2.79 (m, 1H, 2B-H<sub>e</sub>), 2.93 (m, 1H, 4-H<sub>e</sub>), 3.11 (bt, 1H, *J* = 15.2 Hz, 4-H<sub>a</sub>) 3.14 (bt, 1H, *J* = 11 Hz, 3-H), 3.36 (d, 1H, *J* = 9 Hz, 4E-H), 3.49–3.72 (overlap, 4H, 3A-H, 3B-H, 3C-H, and 5A-H), 3.55 (dd, 1H, 9, 8.5 Hz, 4C-H), 3.62 (s, 3H, 1'-OCH<sub>3</sub>), 3.84 (bdd, 1H, *J* = 12.0, 4.5 Hz, 3D-H), 3.93–4.02 (overlap, 4H, 4A-H, 4B-H, 4D-H, 5C-H, and 5D-H), 3.98 (dq, 1H, *J* = 10.0, 6.0 Hz, 5E-H), 4.29 (dq, 1H, *J* = 10.0, 6.0 Hz, 5B-H), 4.76 (bd, 1H, *J* = 10 Hz, 1D-H), 4.86 (d, 1H, *J* = 1.5 Hz, 1'-H), 4.92 (d, 1H, *J* = 11 Hz, 2-H), 5.00 (dd, 1H, *J* = 10, 2 Hz, 1B-H), 5.41 (dd, 1H, *J* = 10, 2 Hz, 1C-H), 5.53 (dd, 1H, *J* = 10, 2 Hz, 1E-H), 5.61 (dd, *J* = 10, 2 Hz, 1A-H), 6.61 (s, 1H, 10-H), and 7.01 (s, 1H, 5-H). <sup>13</sup>C NMR (75.4 MHz, methanol-*d*<sub>4</sub>,  $\delta$ ): 7.1 (7-CH<sub>3</sub>), 15.9 (C-6D), 17.1 (C-6B), 17.3 (C-6C), 17.4 (C-6A), 18.0 (C-6E), 26.3 (3E-CH<sub>3</sub>), 29.7 (C-4), 32.3 (C-2D), 37.1 (C-2A), 37.5 (C-2C), 39.7 (C-2B), 44.6 (C-2E and C-3), 59.6 (1'-OCH<sub>3</sub>), 68.7 (C-4D), 70.7 (C-3E and C-5E), 70.9 (C-3B and C-5D), 72.5 (C-5C and C-5B), 72.9 (C-5A), 75.1 (C-4A), 75.7 (C-4C), 76.2 (C-3D), 76.8 (C-4E), 77.0 (C-2 and C-4B), 79.5 (C-3A), 81.5 (C-3C), 82.2 (C-1'), 97.5 (C-1A), 97.6 (C-1E), 98.8 (C-1B and C-1D), 100.0 (C-1C), 100.1 (C-5), 108.0 (C-8a), 108.6 (C-9a), 111.7 (C-7), 117.2 (C-10), 138.5 (C-4a), 138.7 (C-10a), 159.2 (C-6), 160.5 (C-8), 165.0 (C-9), 176.8 (C-2'), and 198.4 (C-1).

## Acknowledgments

This work was supported by grants of the National Institutes of Health (No. CA091901, to J.R.) and the Spanish Ministry of Science and Technology (BIO97-0771, to J.A.S.) as well as the Plan Regional de Investigación del Principado de Asturias (GE-ME01-05, to J.A.S.). We thank the National Cancer Institute (Bethesda, MD) and Dr. J. Frevert (BioteCon AG, Berlin, Germany) for the antitumor assays, and the referees for helpful discussions.

JA034162H

## References

- Skarbak, J.D.; Speedie, M.K. *Antitumor Compounds of Natural Origin: Chemistry and Biochemistry*. Aszalos, A., editor. Vol. 1. CRC Press; Boca Raton, FL: 1981. p. 191-235.
- Wohlert SE, Künzel E, Machinek R, Méndez C, Salas JA, Rohr J. *J Nat Prod*. 1999; 62:119–121. [PubMed: 9917296]
- Rohr J, Méndez C, Salas JA. *Bioorg Chem*. 1999; 27:41–54.
- Katahira R, Uosaki Y, Ogawa H, Yamashita Y, Nakano H, Yoshida M. *J Antibiot*. 1998; 51:267–274. [PubMed: 9589061]
- Jayasuriya H, Lingham RB, Graham P, Quamina D, Herranz L, Genilloud O, Gagliardi M, Danzeisen R, Tomassini JE, Zink DL, Guan ZQ, Singh SB. *J Nat Prod*. 2002; 65:1091–1095. [PubMed: 12193009]
- Gause, GF. *Antibiotics III—Mechanism of Action of Antimicrobial Antitumor Agents*. Corcoran, JW.; Hahn, FE., editors. Vol. 3. Springer-Verlag; Berlin, New York: 1975. p. 197-202.
- Fox KR, Howarth NR. *Nucleic Acids Res*. 1985; 13:8695–8714. [PubMed: 2934687]
- Sastry M, Patel DJ. *Biochemistry*. 1993; 32:6588–6604. [PubMed: 8329387]
- Sastry M, Fiala R, Patel DJ. *J Mol Biol*. 1995; 251:674–689. [PubMed: 7666419]
- Majee S, Dasgupta D, Chakrabarti A. *Eur J Biochem*. 1999; 260:619–626. [PubMed: 10102989]
- Elias EG, Evans JT. *J Bone Jt Surg, Am Vol*. 1972; 54-A:1730–1736.
- Brown JH, Kennedy BJ. *New Engl J Med*. 1965; 272:111–118. [PubMed: 14224214]

13. Ryan WG, Schwartz TB, Northrop G. *J Am Med Assoc.* 1970; 213:1153–1157.
14. Robins PR, Jowsey J. *J Lab Clin Med.* 1973; 82:576–586. [PubMed: 4271121]
15. Hardman, JG.; Limbird, LE.; Molinoff, PB.; Ruddon, RW.; Goodman Gilman, A., editors. *Goodman & Gilman's The Pharmacological Basis of Therapeutics.* McGraw-Hill; New York, St. Louis, MO: 1996. p. 1267-1268.
16. Silva DJ, Kahne DE. *J Am Chem Soc.* 1993; 115:7962–7970.
17. Silva DJ, Goodnow R Jr, Kahne D. *Biochemistry.* 1993; 32:463–471. [PubMed: 8422355]
18. Gao XL, Mirau P, Patel DJ. *J Mol Biol.* 1992; 223:259–279. [PubMed: 1731073]
19. Lombo F, Blanco G, Fernandez E, Méndez C, Salas JA. *Gene.* 1996; 172:87–91. [PubMed: 8654997]
20. Lombo F, Siems K, Braña AF, Méndez C, Bindseil K, Salas JA. *J Bacteriol.* 1997; 179:3354–3357. [PubMed: 9150235]
21. Lombo F, Braña AF, Méndez C, Salas JA. *J Bacteriol.* 1999; 181:642–647. [PubMed: 9882681]
22. Fernandez E, Weissbach U, Reillo CS, Braña AF, Méndez C, Rohr J, Salas JA. *J Bacteriol.* 1998; 180:4929–4937. [PubMed: 9733697]
23. Rohr J, Weissbach U, Beninga C, Künzel E, Siems K, Bindseil K, Prado L, Lombo F, Braña AF, Méndez C, Salas JA. *Chem Commun.* 1998:437–438.
24. Prado L, Fernandez E, Weissbach U, Blanco G, Quiros LM, Braña AF, Méndez C, Rohr J, Salas JA. *Chem Biol.* 1999; 6:19–30. [PubMed: 9889148]
25. Blanco G, Fernandez E, Fernandez MJ, Braña AF, Weissbach U, Künzel E, Rohr J, Méndez C, Salas JA. *Mol Gen Genet.* 2000; 262:991–1000. [PubMed: 10660060]
26. Fernandez-Lonzano MJ, Remsing LL, Quiros LM, Braña AF, Fernandez E, Sanchez C, Méndez C, Rohr J, Salas JA. *J Biol Chem.* 2000; 275:3065–3074. [PubMed: 10652287]
27. Gonzalez A, Remsing LL, Lombo F, Fernandez MJ, Prado L, Braña AF, Künzel E, Rohr J, Méndez C, Salas JA. *Mol Gen Genet.* 2001; 264:827–835. [PubMed: 11254130]
28. Remsing LL, Garcia-Bernardo J, Gonzalez A, Künzel E, Rix U, Braña AF, Bearden DW, Méndez C, Salas JA, Rohr J. *J Am Chem Soc.* 2002; 124:1606–1614. [PubMed: 11853433]
29. Devereux J, Haerberli P, Smithies O. *Nucleic Acid Res.* 1984; 12:387–395. [PubMed: 6546423]
30. White O, Eisen JA, Heidelberg JF, Hickey EK, Peterson JD, Dodson RJ, Haft DH, Gwinn ML, Nelson WC, Richardson DL, Moffat KS, Qin H, Jiang L, Pamphile W, Crosby M, Shen M, Vamathevan JJ, Lam P, McDonald L, Utterback T, Zalewski C, Makarova KS, Aravind L, Daly MJ, Fraser CM. *Science.* 1999; 286:1571–1577. [PubMed: 10567266]
31. Summers RG, Donadio S, Staver MJ, Wendt-Pienkowski E, Hutchinson CR, Katz L. *Microbiology (Reading, UK).* 1997; 143:3251–3262.
32. Bate N, Butler AR, Smith IP, Cundliffe E. *Microbiology (Reading, UK).* 2000; 146:139–146.
33. Dinur, U.; Hagler, AT. *Reviews in Computational Chemistry.* Lipkowitz, KB.; Boyd, DB., editors. Vol. 2. VCH Publishers; New York: 1991. p. 99-164.
34. Rix U, Fischer C, Remsing LL, Rohr J. *Nat Prod Rep.* 2002; 19:542–580. [PubMed: 12430723]
35. Glycosyltransferase MtmGIV is proposed to be responsible for the attachment of both the first and the last sugar of the trisaccharide unit in MTM. Only the latter activity seems somewhat compromised by the insertional inactivation of MtmW. This might be possible, if the tailoring proteins MtmW (KR) and MtmGIV (GT) arrange themselves close to each other (similar to that in the genetic arrangement), and if only the docking of one set of substrates (alcohol acceptor and NDP-sugar donor) of MtmGIV is slightly affected by the inactivated enzyme MtmW. Note that both proposed substrates for the second glycosyltransfer step are considerably larger than the corresponding substrates of the first glycosyltransfer step.<sup>28</sup>
36. Piel J, Hertweck C, Shipley PR, Hunt DM, Newman MS, Moore BS. *Chem Biol.* 2000; 7:943–955. [PubMed: 11137817]
37. Xiang L, Kalaitzis JA, Nilsen G, Chen L, Moore BS. *Org Lett.* 2002; 4:957–960. [PubMed: 11893195]
38. Montanari A, Rosazza JPN. *J Antibiot.* 1990; 43:883–889. [PubMed: 2117602]
39. Boyd MR. *Princ Pract Oncol.* 1989; 3:1–12.

40. Boyd, MR. Anticancer Drug Development Guide: Preclinical Screening, Clinical Trials, and Approval. Teicher, B., editor. Humana Press, Inc; Totowa, NJ: 1997. p. 23-42.
41. Rabow AA, Shoemaker RH, Sausville EA, Covell DG. J Med Chem. 2002; 45:818–840. [PubMed: 11831894]
42. Frevert, J. personal communication.
43. Ginsburg H, Nissani E, Krugliak M, Williamson DH. Mol Biochem Parasitol. 1993; 58:7–16. [PubMed: 7681547]
44. Givens KT, Kitada S, Chen AK, Rothschilder J, Lee DA. Invest Ophthalmol Visual Sci. 1990; 31:1856–1862. [PubMed: 2145243]
45. Boyd MR. Drug Dev Res. 1995; 34:91–109.
46. NCI-MTM data acquired from the following website. [http://dtp.nci.nih.gov/docs/static\\_pages/compounds/24559.htm](http://dtp.nci.nih.gov/docs/static_pages/compounds/24559.htm)
47. Fernandez E, Weissbach U, Sanchez Reillo C, Braña AF, Méndez C, Rohr J, Salas JA. J Bacteriol. 1998; 180:4929–4937. [PubMed: 9733697]
48. Janssen G, Bibb MJ. Gene. 1993; 124:133–134. [PubMed: 8382652]
49. Aguirrezabalaga I, Olano C, Allende N, Rodriguez L, Braña AF, Méndez C, Salas JA. Antimicrob Agents Chemother. 2000; 44:1266–1275. [PubMed: 10770761]
50. Sambrook, J.; Fritsch, EF.; Maniatis, T. Molecular Cloning. A Laboratory Manual. 2. Cold Spring Harbor Laboratory Press; Cold Spring Harbor, NY: 1989.
51. Kieser, T.; Bibb, MJ.; Buttner, MJ.; Chater, KF.; Hopwood, DA. Practical Streptomyces Genetics. The John Innes Foundation; Norwich, U.K: 2000.
52. Sanger F, Nicklen S, Coulson AR. Proc Natl Acad Sci USA. 1977; 74:5463–5467. [PubMed: 271968]
53. Altschul SF, Gish W, Miller W, Myers EW, Lipman DJ. J Mol Biol. 1990; 215:403–410. [PubMed: 2231712]
54. Altschul SF, Lipman DJ. Proc Natl Acad Sci USA. 1990; 87:5509–5513. [PubMed: 2196570]
55. Altschul SF, Madden TL, Schaffer AA, Zhang JH, Zhang Z, Miller W, Lipman DJ. Nucleic Acid Res. 1997; 25:3389–3402. [PubMed: 9254694]

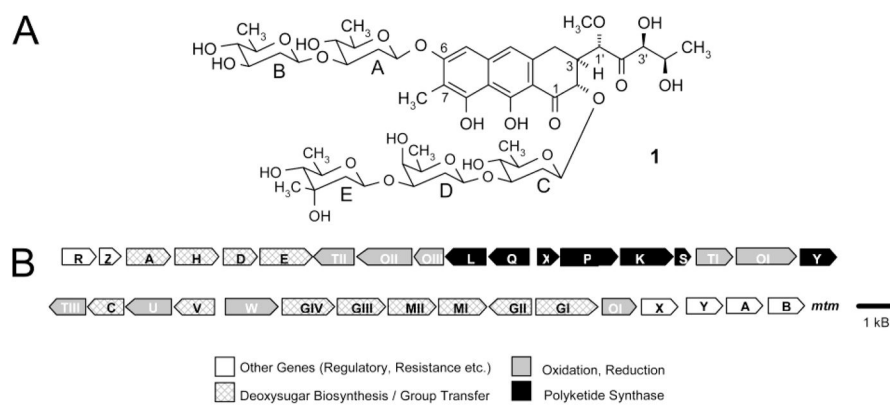


**Figure 1.** (A) Structure of mithramycin (MTM, **1**). (B) Genetic organization of the MTM biosynthetic gene cluster in *S. argillaceus* ATCC 12956.

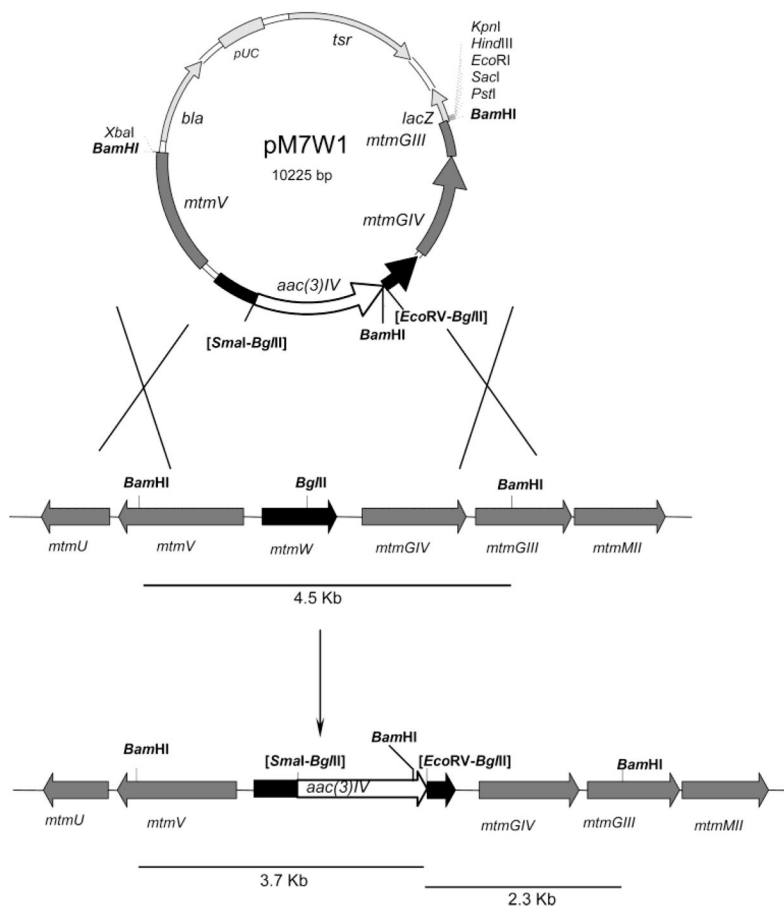
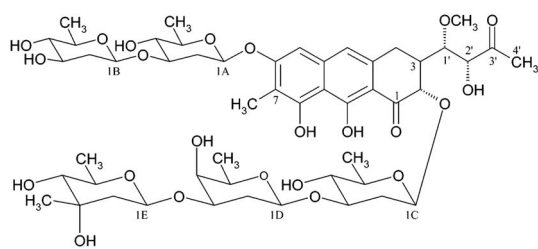
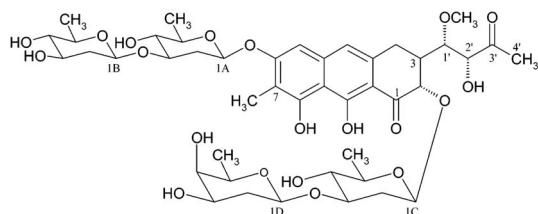


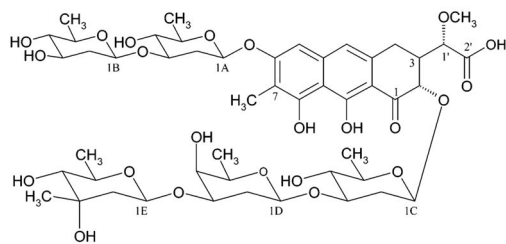
**Figure 2.** Scheme representing the replacement event in the chromosome of wild-type *S. argillaceus* strain by a double crossover to construct mutant M7W1.



Mithramycin SK (2)



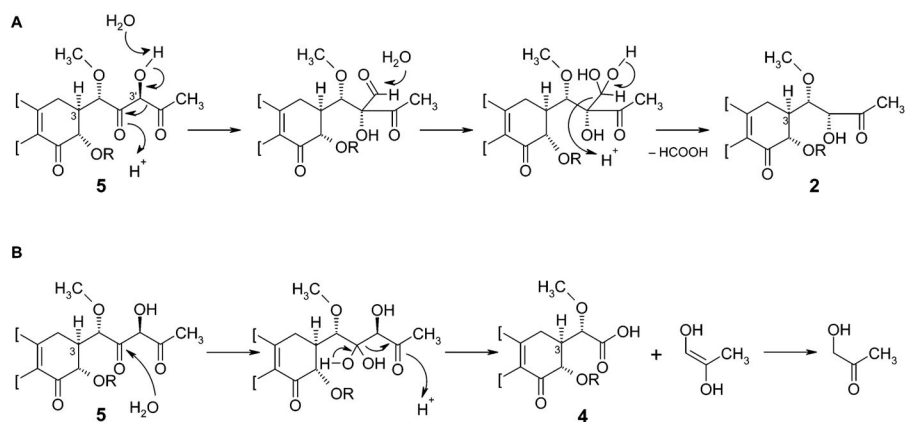
Demycarosyl-mithramycin SK (3)



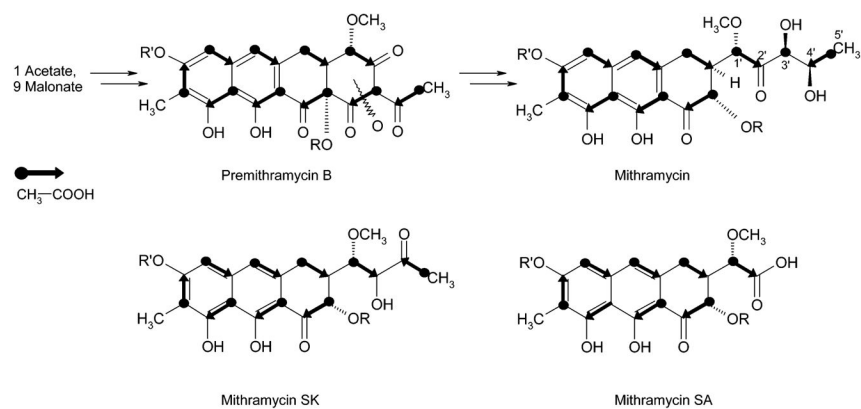
Mithramycin SA (4)

**Figure 3.** Structures of the new metabolites MTM-SK (2), demycarosyl-mithramycin SK (3), and MTM-SA (4) produced by mutant *S. argillaceus* M7W1.





**Figure 4.** Formation of MTM-SK (**2**) and MTM-SA (**4**) through a Favorskii-like rearrangement, and retro-aldol-type cleavage of the reactive product **5**, proposed to be generated by the inactivation of the ketoreductase encoding gene *mtmW*.

**Figure 5.**

Incorporation experiments with  $[1-^{13}\text{C}]$ -acetate and  $[1,2-^{13}\text{C}_2]$ -acetate on the MTM-SK and MTM-SA producer *S. argillaeus* M7W1, compared to the normal incorporation pattern found in MTM (shown above) revealed that the former MTM carbon C-3' and carbons 3',4' and 5', respectively, were excised during the formation of the new metabolites MTM-SK and MTM-SA, respectively. R and R' are the deoxysaccharide chains shown in Figure 1.

Table 1

<sup>1</sup>H and <sup>13</sup>C NMR Analysis of Nonlabeled and Labeled Mithramycin SK (2)

position	<sup>1</sup> H $\delta$ (ppm) <sup>d</sup>	multiplicity <sup>d</sup>	<sup>13</sup> C $\delta$ (ppm) <sup>d</sup>	1- <sup>13</sup> C <sup>b</sup>		<sup>1,2-<sup>13</sup>C<sub>2</sub></sup> <i>J<sub>cc</sub></i> (Hz)
				shift (ppm)	relative enrichments	
1			203.5	197.5	3.0	45
2	4.70 d (11.5)		78.2	78.1		45
3	2.48 overlap		43.7	45.3	3.3	44
4 <sub>a</sub>	3.15 dd (16, 3)		28.3	30.5		44
4 <sub>e</sub>	2.99 overlap					
4 <sub>a</sub>			136.9	139.9	7.7	66
5	6.87 s		101.7	101.3		61
6			159.9	160.3	8.1	69
7			111.0	111.7		69
7-CH <sub>3</sub>	2.15 s		7.9	8.6		
8			156.2	161.9	4.7	61
8 <sub>a</sub>			108.0	108.8		61
9			165.3	177.2	2.7	69
9 <sub>a</sub>			108.5	108.7		69
10	6.89 s		117.0	113.4		66
10 <sub>a</sub>			139.1	140.8	6.2	61
1'	4.25 dd (3.4, 1.5)		78.3	80.7		43
1'-OCH <sub>3</sub>	3.55 s		60.0	60.5		
2'	4.32 d (3.4)		79.5	80.6	6.4	43
3'			209.9	212.6	3.2	39
1A	5.37 dd (10, 2)		97.0			
2A <sub>a</sub>	1.86 ddd (12, 12, 10)		37.5			
2A <sub>e</sub>	2.48 overlap		37.5			
3A	3.78 ddd (12, 9, 5)		81.3			
4A	3.09 dd (9, 9)		75.4			
5A	3.55 overlap		72.6			

position	$^1\text{H } \delta$ (ppm) <sup>a</sup>	multiplicity ( $J_{\text{Hz}}$ )	$^{13}\text{C } \delta$ (ppm) <sup>d</sup>	shift (ppm)	$^{13}\text{C}^b$		$J_{\text{cc}}$ (Hz)
					relative enrichments		
6A (CH <sub>3</sub> )	1.34 d (6)		18.0				
1B	4.75 dd (10, 2)		99.9				
2B <sub>a</sub>	1.59 ddd (12, 12, 10)		40.0				
2B <sub>e</sub>	2.20 ddd (12, 5, 2)		40.0				
3B	3.58 overlap		71.4				
4B	3.01 dd (9, 9)		77.6				
5B	3.41 dq (9, 6)		72.6				
6B (CH <sub>3</sub> )	1.34 d (6)		17.7				
1C	5.14 dd (10, 2)		100.8				
2C <sub>a</sub>	1.62 ddd (12, 12, 10)		37.9				
2C <sub>e</sub>	2.51 ddd (12, 5, 2)		37.9				
3C	3.68 overlap		81.8				
4C	3.05 dd (9, 9)		75.7				
5C	3.33 dq (9, 6)		72.6				
6C (CH <sub>3</sub> )	1.34 d (6)		17.9				
1D	4.70 dd (10, 2)		100.3				
2D <sub>a</sub>	1.80 ddd (12, 12, 10)		32.5				
2D <sub>e</sub>	1.95 ddd (12, 5, 2)		32.5				
3D	3.88 ddd (12, 5, 3)		77.3				
4D	3.72 bs		68.9				
5D	3.70 overlap		71.0				
6D (CH <sub>3</sub> )	1.34 d (6)		16.5				
1E	4.98 dd (9.5, 2)		97.9				
2E <sub>a</sub>	1.56 dd (13, 9.5)		44.3				
2E <sub>e</sub>	1.90 dd (13, 2)		44.3				
3E			70.7				
3E-CH <sub>3</sub>	1.22 s		27.0				
4E	2.99 d (9)		76.8				
5E	3.65 overlap		71.0				

position	$^1\text{H}$ $\delta$ (ppm) <sup>d</sup>	multiplicity ( $J_{\text{Hz}}$ )	$^{13}\text{C}$ $\delta$ (ppm) <sup>d</sup>	shift (ppm)	relative enrichments	$J_{\text{cc}}$ (Hz)
6E (CH <sub>3</sub> )	1.22 d (6)		26.3			
4'	2.35 s		26.3	27.2		39

<sup>a</sup> Data collected in acetone-*d*<sub>6</sub> at 500 MHz ( $^1\text{H}$  NMR) and 125.7 MHz ( $^{13}\text{C}$  NMR).

<sup>b</sup> Data collected in methanol-*d*<sub>4</sub> at 75.4 MHz.

**Table 2**  
Antitumor Analysis Comparing Mithramycin (**1**), Mithramycin SK (**2**), and Demycarosylmthramycin SK (**3**)<sup>a</sup>

	comparison with 2			comparison with 3		
	1	2	1-2 activity improvement factor <sup>e</sup>	3	1-3 activity improvement factor <sup>e</sup>	
	(a) Average log(GI <sub>50</sub> ) Values <sup>b</sup>					
leukemia (5) <sup>c</sup>	-6.65	-7.59	0.94	8.7	-5.55 -1.10	0.08
NSCLC (8) <sup>c</sup>	-6.73	-7.37	0.64	4.4	-5.30 -1.43	0.04
colon (7) <sup>c</sup>	-6.65	-7.32	0.67	4.7	-5.35 -1.30	0.05
CNS (5) <sup>c</sup>	-6.78	-7.61	0.83	6.8	-5.30 -1.48	0.03
melanoma (8) <sup>c</sup>	-6.72	-7.64	0.92	8.3	-5.37 -1.35	0.04
ovarian (6) <sup>c</sup>	-6.60	-7.53	0.93	8.5	-5.23 -1.37	0.04
renal (8) <sup>c</sup>	-6.73	-7.29	0.56	3.6	-5.14 -1.59	0.03
prostate (2) <sup>c</sup>	-6.90	-7.48	0.58	3.8	-5.25 -1.65	0.02
breast (8) <sup>c</sup>	-6.59	-5.89	-0.70	0.2	-5.15 -1.44	0.04
	(b) Average log(IC <sub>50</sub> ) Values <sup>d</sup>					
squamous carcinoma	-5.04	-5.99	0.95	8.9		
melanoma	-5.05	-6.25	1.20	15.8		
lung carcinoma (A549)	-4.92	-6.88	1.96	91.2		
breast carcinoma (MCF-7)	-4.95	-6.74	1.79	61.6		

<sup>a</sup>Data show that **2** exhibits an activity that is up to 90 times higher than that of **1**, whereas **3** is ~25 times less active than **1**.

<sup>b</sup>Average log(GI<sub>50</sub>) values resulting from the sulforhodamine B assay.<sup>40,45,46</sup>

<sup>c</sup>Number in parentheses is the number of cell lines tested in each family.

<sup>d</sup>Average log(IC<sub>50</sub>) values resulting from the neutral red assay.<sup>42</sup>

<sup>e</sup>The activity improvement factor is equal to 10<sup>1-x</sup>, where x is the identifying value for compound **2** or **3**. An activity improvement factor of 1.0 corresponds to no difference in activity.